

## COMMUNICATION

## Chirality imprinting from a chiral guest to the hydrogen bonding network of its hexameric resorcinarene host capsule

Corina H. Pollok,<sup>[a]</sup> Qi Zhang,<sup>[b]</sup> Konrad Tiefenbacher,<sup>[b,c]</sup> and Christian Merten\*<sup>[a]</sup>

**Abstract:** The hexameric capsule of resorcin[4]arene **1** is capable of encapsulating tertiary amines, which has recently successfully been taken advantage of in the application of  $[(\mathbf{1})_6(\text{H}_2\text{O})_8]$  as (co-)catalyst in various asymmetric reactions. However, not much is known about the highly asymmetric but conformationally very dynamic structure of the capsule after uptake of chiral molecules. Therefore, in this contribution, we utilize ECD and VCD spectroscopy to investigate how several chiral guest molecules affect the structural preferences of the capsule  $[(\mathbf{1})_6(\text{H}_2\text{O})_8]$ . In particular, we show that one small chiral amine encapsulated in  $[(\mathbf{1})_6(\text{H}_2\text{O})_8]$  is sufficient to control and dictate the stereochemical preferences of the entire capsule. Furthermore, neither strong  $\pi$ - $\pi$ -interactions nor a significant steric bulk are required for this induction. The observation of such a chiral imprint of the guest's stereochemistry onto its host molecule is expected to have implications also for other supramolecular capsules.

Self-assembled capsules are at the heart of supramolecular chemistry, particularly as they bring together some key challenges: controlled assembly in solution or solid state, recognition of small guest molecules combined with an easily detectable response, and biomimetic catalysis. In the last decades, a variety of architectures have been developed which range from covalent cage structures,<sup>[1]</sup> over metal-ligand capsules,<sup>[2]</sup> to more weakly bound systems held together by hydrogen bonding.<sup>[3]</sup> One very closely investigated system has been first described by Atwood and co-workers, who have discovered the hydrogen bonding driven formation of molecular capsules based on bowl-shaped resorcin[4]arenes.<sup>[4]</sup> In case of the resorcinarene **1** (cf. Figure 1), they observed the formation of a hexameric capsule. This capsule is held together by an extensive hydrogen bonding network, incorporating additional eight water molecules. The importance of the water molecules for the stabilization of the capsule  $[(\mathbf{1})_6(\text{H}_2\text{O})_8]$  has first been concluded from X-ray crystallographic data<sup>[4a]</sup>, and later confirmed by utilizing NMR diffusion measurements.<sup>[4c]</sup>

A closer examination of the crystal structure of  $[(\mathbf{1})_6(\text{H}_2\text{O})_8]$  reveals that each of the six resorcinarenes formally occupies a face of a cube (cf. Figure 1B). The spatial orientation and hydrogen bonding, however,

break the symmetry of the cube, as all resorcin units are slightly tilted in the same direction with respect to the  $C_4$ -symmetry axis of the cube. In Figure 1C, which shows the structure of  $P$ - $[(\mathbf{1})_6(\text{H}_2\text{O})_8]$  optimized at density functional theory (DFT) level,<sup>[5]</sup> the resorcinarenes highlighted in green as well as the other five units show a tilt to the left. The structure with all resorcinarene units tilted to the right corresponds to the enantiomeric  $M$ -structure of the capsule. As there is no chiral bias in the  $[(\mathbf{1})_6(\text{H}_2\text{O})_8]$  capsule, both the  $P$ - and  $M$ -configuration can rapidly interconvert. In addition to their chiral spatial arrangement, the OH $\cdots$ O hydrogen bonding patterns of four of the resorcinarene units feature a chiral orientation:<sup>[4a]</sup> they are either all pointing clockwise (*cw*) or counter-clockwise (*ccw*) around the rim of the resorcinarene ( $C_4$  symmetry), while both right and left handed **1** are equally present in the capsule. The remaining two monomer units feature an achiral hydrogen bonding network ( $C_{2v}$  symmetry). Hence, the  $[(\mathbf{1})_6(\text{H}_2\text{O})_8]$  capsule is a highly asymmetric, yet structurally very dynamic supramolecular system.

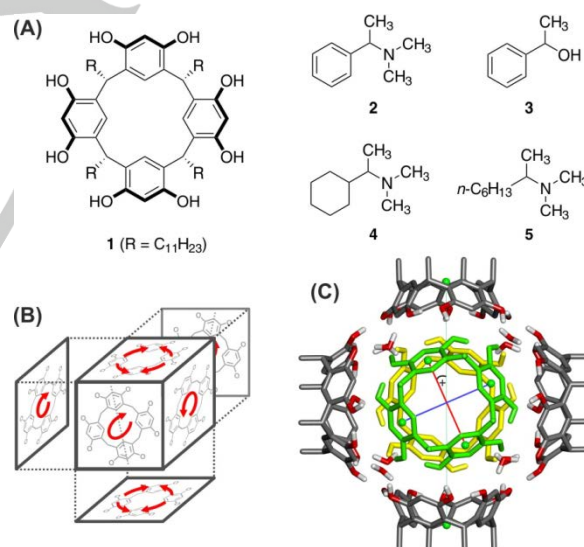


**Figure 1.** (A) Structure of the capsule building block (**1**), and the four investigated chiral guest molecules (**2-5**); (B) Cube-view of the capsule; (C) three-dimensional view of the hexameric capsule  $[(\mathbf{1})_6(\text{H}_2\text{O})_8]$ ;

[a] C. H. Pollok, Dr. C. Merten  
Ruhr-Universität Bochum  
Fakultät für Chemie und Biochemie, Organische Chemie 2  
Universitätsstraße 150, 44801 Bochum, Germany  
E-mail: christian.merten@ruhr-uni-bochum.de

[b] Dr. Q. Zhang, Prof. Dr. K. Tiefenbacher  
Department of Chemistry, University of Basel, St. Johannis-Ring 19,  
CH-4056 Basel, Switzerland

[c] Prof. Dr. K. Tiefenbacher  
Department of Biosystems Science and Engineering, ETH Zürich,  
Mattenstrasse 26, CH-4058 Basel, Switzerland

Supporting information for this article is given via a link at the end of the document.

The observation of the encapsulation of tetraalkylammonium<sup>[6]</sup> salts into the hexameric resorcinarene capsule via cation- $\pi$  interactions triggered the interest in studying them as cavities for catalytic applications.<sup>[7]</sup> In this context,  $[(\mathbf{1})_6(\text{H}_2\text{O})_8]$  was found to be a highly substrate selective catalyst for a variety of reactions,<sup>[8]</sup> including enantioselective iminium-catalysed 1,4-reduction. In several of these reactions, the capsule acts as Brønsted acid, so that the strong interaction of the capsule with the encapsulated substrates such as trialkylamines is

## COMMUNICATION

assumed to be related to cation- $\pi$  stabilization between the resulting ammonium ion and the capsule walls.<sup>[8h]</sup>

While the uptake of guest molecules into  $[(\mathbf{1})_6(\text{H}_2\text{O})_8]$  can easily be monitored by  $^1\text{H-NMR}$  spectroscopy, not much is known about the influence of the guest on the structural preferences of the capsule. This is in stark contrast to other cage compounds such as coordination cages, for which it could be shown that the encapsulation of a chiral guest can efficiently induce preferred chiral structures to the host, which even persists after removal of the guest.<sup>[9]</sup> In case of  $[(\mathbf{1})_6(\text{H}_2\text{O})_8]$ , due to the dynamic nature of the hydrogen-bond based assembly any potentially guest induced stereochemistry would be lost upon guest exchange. However, does this imply that the hydrogen bonding network of the capsule is also too dynamic to allow the formation of a preferred chiral superstructure in solution? In order to answer this question, we herein utilize chiroptical spectroscopies to investigate the encapsulation of chiral guest molecules in  $[(\mathbf{1})_6(\text{H}_2\text{O})_8]$ .

As starting point for our investigation, we prepared mixtures of **1** and enantiopure tertiary amine **2** in water-saturated  $[\text{D}_1]$ chloroform in different ratios.<sup>[10]</sup> Figure 2A shows the electronic circular dichroism (ECD) spectra recorded for seven different mixtures, which all reveal a strong positive Cotton effect at 304 nm and a negative Cotton effect at 287 nm upon addition of (*S*)-**2**. These Cotton effects strongly suggest that the interactions between the encapsulated protonated amine and the deprotonated capsule are indeed strong enough to impose a preferred handedness onto the entire capsule structure. In order to confirm that the observed ECD spectral pattern is due to an induction of a stereochemical preference into the capsule, and that the amine does not simply form hydrogen bonded adducts with the host, the experiments have been repeated in water-free solvent. As expected, if the water necessary for the stabilization of the capsule is removed, no induced ECD is observed.

Interestingly, with increasing concentration of the guest, the intensities of the ECD bands first increase until a plateau is reached for ratios of about 1:3 to 1:6. Upon further addition of guest molecules, the ECD intensities slowly decrease. This trend correlates qualitatively with the number of encapsulated guest molecules **2** determined based on  $^1\text{H-NMR}$  titration experiments (Figure 2B), which again supports the conclusion that the encapsulated guest influences the stereochemistry of the host superstructure.

It should be noted that the alcohol **3** and other chiral molecules have previously been reported to induce a similar ECD signature to the  $\pi$ - $\pi^*$  transitions of **1**.<sup>[11]</sup> However, at the time of that study, the possible formation of hexameric capsules was not known yet. Therefore, in contrast to the present study, the experiments required significantly higher concentrations of the chiral dopants. Furthermore, they have been carried out using water-free solvents, so that a formation of a capsule was suppressed. Under our experimental conditions, i.e. when using water-saturated solvent, alcohol **3** does not show any ECD induction (cf. SI).

In case of alcohol **3**, the reported induced ECD was explained with an incorporation of the OH group in the hydrogen bonding network along the rim of the resorcinarene, which causes a local symmetry breaking and thus an exciton coupling effect. In case of capsule  $[(\mathbf{1})_6(\text{H}_2\text{O})_8]$ , a similar mechanism of symmetry breaking could be in effect, in which the desymmetrization is caused by the chiral arrangement of the adjacent resorcinarene units. However, an empirical analysis of the exciton coupling pattern is not possible, so that we

attempted to use TDDFT calculations to predict the ECD spectrum of *P*- $[(\mathbf{1})_6(\text{H}_2\text{O})_8]$ . Unfortunately, due to the size of the molecule, and even after truncation of the undecyl groups, the calculations never finished successfully, so that we turned to another chiroptical technique for the determination of the configuration respectively chiral conformation of (*S*)-**2**@ $[(\mathbf{1})_6(\text{H}_2\text{O})_8]$ .

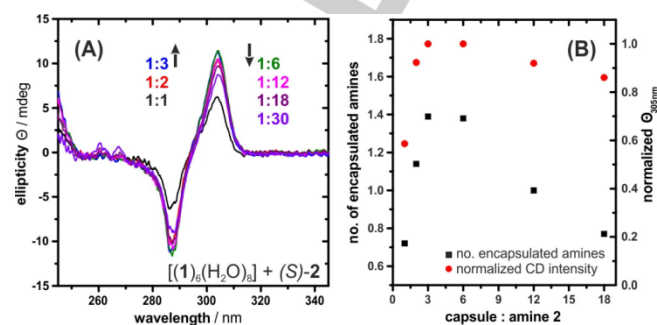


**Figure 2.** (A) ECD spectra of mixtures of  $[(\mathbf{1})_6(\text{H}_2\text{O})_8]$  with (*S*)-**2** in water-saturated  $[\text{D}_1]$ -chloroform. (B) Correlation of the normalized ellipticity of the first Cotton effect ( $\lambda = 304$  nm) and the number of encapsulated amines with the capsule:amine ratio (concentration of **1** = 0.1 mM; 10 mm pathlength).

Vibrational circular dichroism (VCD) spectroscopy, the chiral version of infrared spectroscopy, measures the differential absorbance of left- and right-circularly polarized infrared light during a vibrational transition. Hence, it does not rely on the presence of certain chromophores, but each IR active vibrational mode of a chiral molecule gives rise to a VCD band. While VCD spectroscopy finds its main applications in the determinations of absolute configurations,<sup>[12]</sup> it has also become an interesting tool to study solvation effects<sup>[13]</sup> or chirality transfer phenomena,<sup>[14]</sup> and it has been shown to be applicable to larger molecular assemblies, ranging from regular helical polymers<sup>[15]</sup> to cryptophanes,<sup>[16]</sup> and should thus be the ideal technique for the characterization of the chiral cage structure.

The IR and VCD spectra were recorded for mixtures of the capsule with both enantiomers of **2** at the ratio of maximum encapsulation (1:6). The obtained spectra are shown in Figure 3, which also provides the IR and VCD spectra of the pure guest molecule **2** for comparison.<sup>[17]</sup> It becomes immediately apparent that the main contributions to the IR spectrum arise from the hexameric capsule as the band intensities of **2** are approximately five times weaker than those of the host. Due to the size of the capsule and the complexity of the vibrational modes, detailed assignments of bands to specific vibrational modes are very difficult, even when considering the spectra calculations discussed below. Nevertheless, some assignments could be made by comparison with band assignment tables and by visual comparison of the animated vibrations:<sup>[18]</sup> band 2 originates mainly from C=C stretching modes, bands 3/4 arise from bending modes of the aromatic C-H (in-plane), band 5 and bands 7-10 from deformation vibrations of the aliphatic  $\text{CH}_2/\text{CH}_3$ , while band 6 has mainly contributions from (hydrogen bonded) OH group.

In contrast to the IR spectrum, the VCD spectra of the enantiomeric mixtures feature many sharp and well resolved bands. All observed VCD spectral features can clearly be assigned to absorbance bands in the parent IR spectrum, and even the water bending mode (band 1) appears

## COMMUNICATION

to feature VCD activity. It can therefore be concluded, that the obtained VCD spectra also originate from a chiral hexameric capsule structure. This conclusion is further supported by comparison with the VCD spectrum of the pure amine **2**, which is generally much weaker in intensity. Solely two relatively strong bands of **2** at 1451 and 1096  $\text{cm}^{-1}$  might interfere with the VCD spectral signatures of the capsule. However, careful comparison of the experimental spectra reveals that the spectrum of the mixture  $[(\mathbf{1})_6(\text{H}_2\text{O})_8]/(\text{S})\text{-}\mathbf{2}$  features a negative band at 1450  $\text{cm}^{-1}$  whereas a positive band is observed in the spectrum of pure (S)-**2**. Similarly, the interference of the band at 1096  $\text{cm}^{-1}$  is also negligible. The VCD band 2 (1650–1580  $\text{cm}^{-1}$ ) provides another support for the conclusion that the VCD spectral signature arises from the host molecule, as the amine does not feature any bands in the IR/VCD spectra within this range.

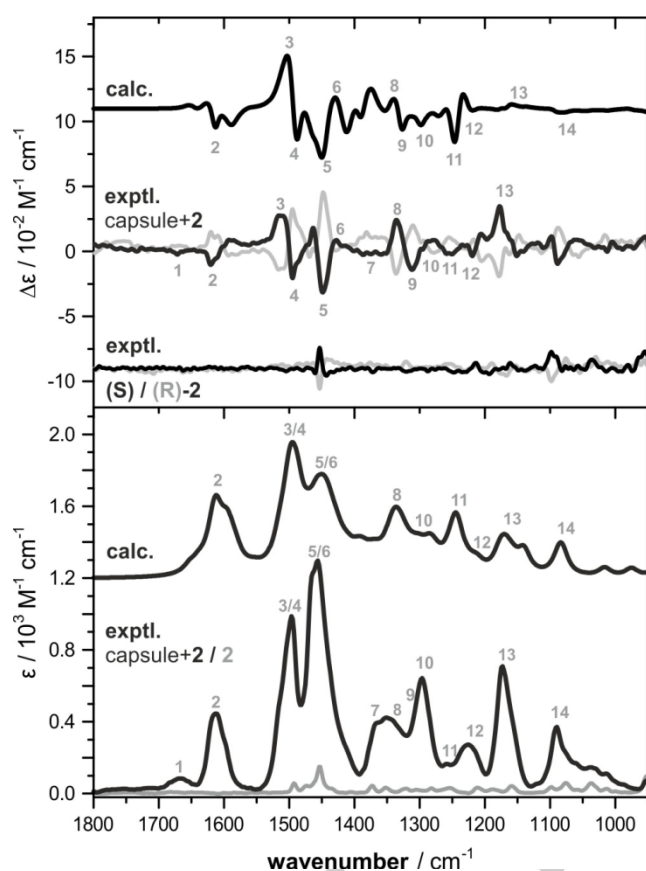


**Figure 3.** Comparison of experimental IR (bottom) and VCD (top) spectra of a 1:6 mixture of capsule  $[(\mathbf{1})_6(\text{H}_2\text{O})_8]$  and amine **2** with calculated spectra of the *P*-capsule (B3LYP/6-31G(d,p)). (S) and (R) refer to the configuration of the amine, while the numbers indicate band assignments. The spectra were taken at a concentration of 45 mM in water-saturated  $[\text{D}_1\text{-}]\text{-chloroform}$ .

The experimental spectra provide clear evidence for the induction of a chiral conformation to the capsule structure. However, the handedness of the conformation can also not be determined directly from the VCD spectra, so that DFT-based spectra calculations were attempted once more. As vibrational spectra calculations do not require the computation of electronic excitations, the choice of a very small basis set finally allowed the successful completion of the frequency analysis

for a methyl-truncated  $[(\mathbf{1})_6(\text{H}_2\text{O})_8]$  for several protonation and hydrogen bonding states. However, the predicted fingerprint range of the IR and VCD spectra were found to be insensitive to the protonation state or the orientation of the connecting water molecules, and even the inclusion of (S)- or (R)-amine in the capsule did not affect the computed spectral pattern (cf. Fig. S3). This insensitivity to minor structural changes suggests that any other small conformational change or solute-solvent interaction occurring in solution, which are neglected in the calculation, should also not significantly influence the outcome of the calculations.

Alongside the experimental data, Figure 3 shows a representative set of theoretical spectra obtained for *P*- $[(\mathbf{1})_6(\text{H}_2\text{O})_8]$ . On first sight, an unambiguous band assignment between the experimental and computed IR spectra (cf. Figure 3, bottom) can only be made for bands 2–6, as the range from bands 7–13 features a somewhat different intensity distribution. In particular the range around IR band 7 appears to be significantly less intense in the calculations. Therefore, in order to also computationally confirm that the observed IR spectra arise from a capsule structure, we calculated the IR spectrum of a single resorcinarene molecule. As expected, the direct comparison of monomer and hexameric supramolecular aggregate is in clear favour for the spectrum of the capsule (cf. Fig. S4). A presumable cause for the remaining disagreement might be the necessary neglect of the 24 undecyl chains and their substitution with methyl groups. Thereby, the contributions of hundreds of  $\text{CH}_2$  deformation and C–C stretching modes, which would be expected to appear in the spectral range from 1350–1000  $\text{cm}^{-1}$ , could not be considered at all. Consequently, the agreement in the lower frequency range of the VCD spectra is also affected (cf. Figure 3, top), but the overall comparison allows the assignment of significantly more bands. In particular, the VCD spectral pattern between 1550–1400  $\text{cm}^{-1}$  (bands 3–6) can be concluded to be highly characteristic for the configuration of the capsule, which is further supported by the spectra calculations for other capsule structures (cf. Fig. S3). Therefore, the VCD spectra in the range of the aromatic CH-in plane and OH deformation modes provide the highest analytical value, and consequently confirms that the capsule adopts a *P*-configuration upon encapsulation of (S)-**2**.

To further explore whether the successful induction of chirality is solely governed by cation- $\pi$  and coulomb interactions, or if the aromatic nature of the side group of the chiral amine may also play a role, we prepared the amine **4** from the commercially available primary amine.<sup>[19]</sup> We thus removed the possible influence of  $\pi$ - $\pi$  interactions while simultaneously slightly increasing the conformational rigidity of the side group.<sup>[20]</sup> The VCD spectra, however, do not indicate any noteworthy spectral changes (cf. Fig. S1), so that it can be concluded that additional  $\pi$ - $\pi$  interactions do not seem to play a key role in the induction process. An influence of the bulky six-membered ring could also be excluded by recording spectra of equimolar mixtures of  $[(\mathbf{1})_6(\text{H}_2\text{O})_8]/\mathbf{5}$ , which showed the same induced VCD signatures. It is worth noting that the (S)-enantiomers of all three evaluated amines **2**, **4**, and **5** induce the same VCD spectral signature to the vibrational modes of  $[(\mathbf{1})_6(\text{H}_2\text{O})_8]$ , suggesting that the three-dimensional shape of the guest molecule determines the handedness of the capsule.

Concluding this study, it can be stated that a single chiral cationic guest molecule can indeed impose stereochemical preferences onto the hydrogen bonding network of the resorcinarene capsule  $[(\mathbf{1})_6(\text{H}_2\text{O})_8]$ . While such chiral capsules could not be isolated, or even prepared



without a chiral guest molecule, combining the strengths of different chiroptical spectroscopies successfully lead to an unambiguously proof of the induction of chirality. Moreover, this study constitutes the first application of VCD spectroscopy for the investigation of the stereochemical communication between an achiral supramolecular capsule and its chiral guest molecule. Guided by the corresponding DFT based spectra calculations, it even allowed the determination of the preferred handedness of the hydrogen bonding network. We believe that these observations are an important milestone not only for a better understanding of supramolecular structure formation, but that it might also stimulate further studies on enhanced enantioselectivities of asymmetric catalysis in these and other capsules.<sup>[8b]</sup> In order to develop a more general perspective on the observability of such chirality imprinting events, we are currently investigating other chiral and achiral capsules and their structural changes upon encapsulations of guest molecules by VCD spectroscopy.

## Experimental Details.

The resorcin[4]arene **1** and the amines **4** and **5** were prepared according to previously reported procedures.<sup>[19, 21]</sup> Amine **2** and all other chemicals were purchased from Sigma Aldrich and used without further purification. Water-saturated chloroform-d<sub>1</sub> was prepared by vigorously stirring a mixture of distilled water and chloroform-d<sub>1</sub> for one day followed by phase separation if necessary.

The IR and VCD spectra were recorded in the fingerprint region (1800–950 cm<sup>-1</sup>) on a Bruker Vertex 70v FT-IR spectrometer equipped with a Bruker PMA 50 module for VCD measurements (spectral resolution: 4 cm<sup>-1</sup>, PEM frequency: 1500 cm<sup>-1</sup>). The samples were held in a sealed BaF<sub>2</sub> cell with a pathlength of 100 μm, and about 40000 scans have been averaged for the VCD spectra over the course of 8 hrs. The baselines of the VCD spectra were corrected by subtraction of the spectrum of the racemic mixture. UV and ECD spectra were recorded on a Jasco J-815 spectrometer.

Geometry optimizations were performed in the DFT framework at the B3LYP/6-31G(2d,p) level of theory with the Gaussian 09 Rev. D program package.<sup>[22]</sup> The calculations were carried out for a truncated capsule, in which all 24 undecyl chains were substituted by methyl groups. The IR and VCD spectra calculations had to be performed with the slightly smaller 6-31G(d,p) basis set, as all attempts to use the almost negligible larger basis led to repeated sudden crashes of the calculations. Hence, the frequency analysis showed small imaginary frequencies (<10 cm<sup>-1</sup>). For better comparison with the experimental data, and to account for errors arising from the harmonic approximation, the calculated wavenumbers were scaled by a factor of 0.96. Vibrational line broadening was simulated by assigning a Lorentzian band shape of 12 cm<sup>-1</sup> half-width at half-height (HWHH) to the calculated dipole and rotational strength.

## Acknowledgements

C.M. thanks the Fonds der Chemischen Industrie for a Liebig fellowship and acknowledges support by the Deutsche Forschungsgemeinschaft through the Cluster of Excellence RESOLV (“Ruhr Explores SOLVation”, EXC 1069) and the Research Department IFSC (“Interfacial Systems Chemistry”) of the Ruhr University Bochum for

access to the CD spectrometer. K.T. acknowledges the support from the European Research Council Horizon 2020 Programme (ERC Starting grant 714620-TERPENECAT), the Swiss National Science Foundation as part of the NCCR Molecular Systems Engineering and the Bayerische Akademie der Wissenschaften (Junges Kolleg).

**Keywords:** chirality • circular dichroism • molecular capsules • vibrational spectroscopy • vibrational optical activity

- a) A. J. Kirby, *Angew. Chem. Int. Ed.* **1996**, *35*, 706-724; b) R. Breslow, S. D. Dong, *Chem. Rev.* **1998**, *98*, 1997-2012; c) J. K. M. Sanders, *Chem. Eur. J.* **1998**, *4*, 1378-1383; d) W. B. Motherwell, M. J. Bingham, Y. Six, *Tetrahedron* **2001**, *57*, 4663-4686; e) D. M. Vriezema, M. Comellas Aragonès, J. A. A. W. Elemans, J. J. L. M. Cornelissen, A. E. Rowan, R. J. M. Nolte, *Chem. Rev.* **2005**, *105*, 1445-1490; f) K. T. Holman, in *Encyclopedia of Supramolecular Chemistry*, Taylor & Francis, **2007**, pp. 340-348; g) G. Zhang, M. Mastalerz, *Chem. Soc. Rev.* **2014**, *43*, 1934-1947.
- a) M. D. Pluth, R. G. Bergman, K. N. Raymond, *Acc. Chem. Res.* **2009**, *42*, 1650-1659; b) M. Yoshizawa, J. K. Klosterman, M. Fujita, *Angew. Chem. Int. Ed.* **2009**, *48*, 3418-3438; c) T. K. Ronson, S. Zarra, S. P. Black, J. R. Nitschke, *Chem. Commun.* **2013**, *49*, 2476-2490; d) M. Han, D. M. Engelhard, G. H. Clever, *Chem. Soc. Rev.* **2014**, *43*, 1848-1860; e) C. J. Brown, F. D. Toste, R. G. Bergman, K. N. Raymond, *Chem. Rev.* **2015**, *115*, 3012-3035; f) S. H. A. M. Leenders, R. Gramage-Doria, B. de Bruin, J. N. H. Reek, *Chem. Soc. Rev.* **2015**, *44*, 433-448.
- a) J. Rebek, *Acc. Chem. Res.* **2009**, *42*, 1660-1668; b) D. Ajami, J. Rebek, *Acc. Chem. Res.* **2013**, *46*, 990-999; c) D. Ajami, L. Liu, J. Rebek Jr, *Chem. Soc. Rev.* **2015**, *44*, 490-499.
- a) L. R. MacGillivray, J. L. Atwood, *Nature* **1997**, *389*, 469-472; b) J. L. Atwood, L. J. Barbour, A. Jerga, *PNAS* **2002**, *99*, 4837-4841; c) L. Avram, Y. Cohen, *Org. Lett.* **2002**, *4*, 4365-4368; d) L. Avram, Y. Cohen, J. Rebek Jr, *Chem. Commun.* **2011**, *47*, 5368-5375.
- We define P-chirality to this structure in analogy to the definition of axial chirality: The smallest angle between the connecting line of phenyl centroids with the former cube symmetry axis is positive.
- a) A. Shivanyuk, J. Rebek, *PNAS* **2001**, *98*, 7662-7665; b) L. Avram, Y. Cohen, *J. Am. Chem. Soc.* **2002**, *124*, 15148-15149.
- a) G. Borsato, A. Scarso, in *Organic Nanoreactors*, Academic Press, Boston, **2016**, pp. 203-234; b) L. Catti, Q. Zhang, K. Tiefenbacher, *Chem. Eur. J.* **2016**, *22*, 9060-9066; c) L. Catti, Q. Zhang, K. Tiefenbacher, *Synthesis* **2016**, *48*, 313-328.
- a) G. Bianchini, G. L. Sorella, N. Canever, A. Scarso, G. Strukul, *Chem. Commun.* **2013**, *49*, 5322-5324; b) Q. Zhang, K. Tiefenbacher, *J. Am. Chem. Soc.* **2013**, *135*, 16213-16219; c) S. Giust, G. La Sorella, L. Sporni, F. Fabris, G. Strukul, A. Scarso, *Asian Journal of Organic Chemistry* **2015**, *4*, 217-220; d) Zhang Q, Tiefenbacher K, *Nat Chem* **2015**, *7*, 197-202; e) L. Catti, K. Tiefenbacher, *Chem. Commun.* **2015**, *51*, 892-894; f) G. La Sorella, L. Sporni, G. Strukul, A. Scarso, *ChemCatChem* **2015**, *7*, 291-296; g) G. L. Sorella, L. Sporni, G. Strukul, A. Scarso, *Adv. Syn. Cat.* **2016**, *358*, 3443-3449; h) T. M. Bräuer, Q. Zhang, K. Tiefenbacher, *Angew. Chem. Int. Ed.* **2016**, *55*, 7698-7701; i) G. La Sorella, L. Sporni, P. Ballester, G. Strukul, A. Scarso, *Catalysis Science & Technology* **2016**, *6*, 6031-6036; j) T. Caneva, L. Sporni, G. Strukul, A. Scarso, *RSC Advances* **2016**, *6*, 83505-83509; k) L. Catti, A. Pöthig, K. Tiefenbacher, *Adv. Syn. Cat.* **2017**, n/a-n/a.
- A. J. Terpin, M. Ziegler, D. W. Johnson, K. N. Raymond, *Angew. Chem. Int. Ed.* **2001**, *40*, 157-160.
- It is important to note, that an equimolar mixture of **1** and **2** equals to a host/guest ratio of 1:6 upon self-assembly of the hexameric supramolecular structure in solution. Throughout the manuscript, we will refer to the host/guest ratio as the ratio of capsule [(1)<sub>6</sub>(H<sub>2</sub>O)<sub>6</sub>] to guest molecules in order to avoid confusion.
- K. Kobayashi, Y. Asakawa, Y. Kikuchi, H. Toi, Y. Aoyama, *J. Am. Chem. Soc.* **1993**, *115*, 2648-2654.
- a) M. A. Munoz, A. Urzua, J. Echeverria, M. A. Bucio, A. Hernandez-Barragan, P. Joseph-Nathan, *Phytochemistry* **2012**, *80*, 109-114; b) C. Merten, V. Smyrniotopoulos, D. Tasdemir, *Chem. Commun.* **2015**, *51*, 16217-16220; c) L. G. Felipe, J. M. Batista, Jr., D. C. Baldoqui, I. R. Nascimento, M. J. Kato, Y. He, L. A. Nafie, M. Furlan, *Org. Biomol. Chem.* **2012**, *10*, 4208-4214; d) E. D. Gussem, P. Bultinck, M. Feledziak, J. Marchand-Brynaert, C. V. Stevens, W. Herrebout, *Phys. Chem. Chem. Phys.* **2012**; e) R. F. Sprenger, S. S. Thomasi, A. G. Ferreira, Q. B. Cass, J. M. Batista Junior, *Org. Biomol. Chem.* **2016**, *14*, 3369-3375.
- a) M. R. Poopari, Z. Dezhahang, Y. Xu, *Phys. Chem. Chem. Phys.* **2013**, *15*, 1655-1665; b) C. Merten, R. McDonald, Y. Xu, *Inorg. Chem.* **2014**, *53*, 3177-3182; c) N. M. Kreienborg, C. H. Pollok, C. Merten, *Chem. Eur. J.* **2016**, *22*, 12455-12463.

- [14] a) E. Debie, L. Jaspers, P. Bultinck, W. Herrebout, B. V. D. Veken, *Chem. Phys. Lett.* **2008**, *450*, 426-430; b) C. Merten, Y. Xu, *Angew. Chem. Int. Ed.* **2013**, *52*, 2073-2076; c) C. Merten, C. H. Pollok, S. Liao, B. List, *Angew. Chem. Int. Ed.* **2015**, *54*, 8841-8845.
- [15] a) S. R. Domingos, S. J. Roeters, S. Amirjalayer, Z. Yu, S. Hecht, S. Woutersen, *Phys. Chem. Chem. Phys.* **2013**, *15*, 17263-17267; b) H.-Z. Tang, B. M. Novak, J. He, P. L. Polavarapu, *Angew. Chem.* **2005**, *117*, 7464-7467; c) C. Merten, A. Hartwig, *Macromolecules* **2010**, *43*, 8373-8378; d) C. Merten, J. F. Reuther, J. D. DeSousa, B. M. Novak, *Phys. Chem. Chem. Phys.* **2014**, *16*, 11456-11460.
- [16] a) T. Brotin, D. Cavagnat, J. P. Dutasta, T. Buffeteau, *J. Am. Chem. Soc.* **2006**, *128*, 5533-5540; b) T. Brotin, N. Daugey, N. Vanthuynne, E. Jeanneau, L. Ducasse, T. Buffeteau, *J. Phys. Chem. B* **2015**.
- [17] C. Merten, M. Amkreutz, A. Hartwig, *Chirality* **2010**, *22*, 754-761.
- [18] G. Socrates, *Infrared and Raman Characteristic Group Frequencies*, 3rd ed., John Wiley & Sons, Ltd., **2001**.
- [19] D. Casarini, S. Davalli, L. Lunazzi, D. Macciantelli, *J. Org. Chem.* **1989**, *54*, 4616-4619.
- [20] C. H. Pollok, C. Merten, *Phys. Chem. Chem. Phys.* **2016**, *18*, 13496 - 13502.
- [21] L. M. Tunstad, J. A. Tucker, E. Dalcaneale, J. Weiser, J. A. Bryant, J. C. Sherman, R. C. Helgeson, C. B. Knobler, D. J. Cram, *J. Org. Chem.* **1989**, *54*, 1305-1312.
- [22] *Gaussian 09, Revision D.01*, M. J. Frisch, G. W. Trucks, H. B. Schlegel, G. E. Scuseria, M. A. Robb, J. R. Cheeseman, G. Scalmani, V. Barone, B. Mennucci, G. A. Petersson, H. Nakatsuji, M. Caricato, X. Li, H. P. Hratchian, A. F. Izmaylov, J. Bloino, G. Zheng, J. L. Sonnenberg, M. Hada, M. Ehara, K. Toyota, R. Fukuda, J. Hasegawa, M. Ishida, T. Nakajima, Y. Honda, O. Kitao, H. Nakai, T. Vreven, J. J. A. Montgomery, J. E. Peralta, F. Ogliaro, M. Bearpark, J. J. Heyd, E. Brothers, K. N. Kudin, V. N. Staroverov, T. Keith, R. Kobayashi, J. Normand, K. Raghavachari, A. Rendell, J. C. Burant, S. S. Iyengar, J. Tomasi, M. Cossi, N. Rega, J. M. Millam, M. Klene, J. E. Knox, J. B. Cross, V. Bakken, C. Adamo, J. Jaramillo, R. Gomperts, R. E. Stratmann, O. Yazyev, A. J. Austin, R. Cammi, C. Pomelli, J. W. Ochterski, R. L. Martin, K. Morokuma, V. G. Zakrzewski, G. A. Voth, P. Salvador, J. J. Dannenberg, S. Dapprich, A. D. Daniels, O. Farkas, J. B. Foresman, J. V. Ortiz, J. Cioslowski, D. J. Fox, Wallingford CT, **2013**

COMMUNICATION

---

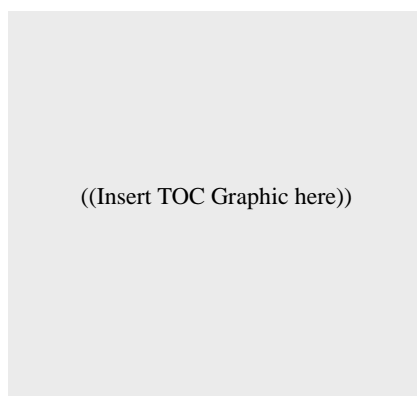
**Entry for the Table of Contents** (Please choose one layout)

Layout 1:

**COMMUNICATION**

---

Text for Table of Contents

*Author(s), Corresponding Author(s)\****Page No. – Page No.****Title**

Layout 2:

**COMMUNICATION**

---

A large grey rectangular box containing the text "((Insert TOC Graphic here))".

*Author(s), Corresponding Author(s)\****Page No. – Page No.****Title**Text for Table of Contents

---